

Self Assembled Quantum Dot Mid-infrared Si/Ge Photodetector Fabricated by Pulsed Laser Deposition

MOHAMMED S. HEGAZY, TAMER F. REFAAT, and HANI E. ELSAYED-ALI*

Applied Research Center
Old Dominion University
12050 Jefferson Avenue
Newport News, VA 23606
UNITED STATES

Abstract: A Multilayered mid-infrared Si/Ge quantum-dot photodetector is fabricated by pulsed laser deposition. Forty successive Ge quantum dot layers, each covered with a thin Si layer, are deposited. Deposition was monitored by *in situ* reflection-high energy electron diffraction. The size distribution of the quantum dots was characterized by *ex situ* atomic force microscopy. I-V measurements reveal typical diode characteristics, while responsivity measurements show an absorption peak around 2 μm wavelength. Noise variation with applied voltage and corresponding detectivity were also measured.

Key-Words: Quantum dots; Si/Ge; infrared detectors; optoelectronic devices

1. Introduction

Devices that are based on Si/Ge quantum dots (QD) have received significant attention in the past few years. Ge QD have been proven to be promising for fabricating infrared (IR) photodetectors [1,2], thermoelectric devices [3], and enhancing the performance of solar cells [4]. QD infrared photodetectors (QIPD) were first proposed by Ryzhii in 1996 [5] and were shown to have better sensitivity to normal incidence photoexcitation, broader IR response, high photoconductive gain, high extraction efficiency, lower dark current, elevated operation temperatures, and higher photoelectric gain than quantum well infrared photodetectors (QWPD) [6-8]. Unlike the case of single crystal photodetectors, controlling the QD material composition, size distribution, spatial distribution, shape and density can be used to tune the device detection band and to control the spectral response of the QDIP in a broad range throughout the IR region [1,6,9].

A typical QDIP device consists of a multiple of two-dimensional arrays of QDs separated by spacing layers and sandwiched between two heavily doped layers: emitter and

collector. The device can have different junction structures. In most cases, QDs are grown via self-assembly in lattice mismatched semiconductors, e.g. Si/Ge and InGaAs/GaAs. Ge growth on Si follows the Stranski-Krastanow mode, in which Ge atoms form few epitaxial monolayers (wetting layer) before developing self-assembled QDs, in order to relief the strain caused by the lattice mismatch [10]. The amount of that strain and deposition conditions control the shape, size and spatial distributions of the QDs; therefore allows for the tuneability of the detected wavelength band.

Ge QDs were grown on Si by molecular beam epitaxy (MBE) [11], chemical vapor deposition (CVD) [12], and liquid phase epitaxy (LPE) [2]. However, very few works have used pulsed laser deposition (PLD) to grow Ge on Si. Among the attractive features of PLD are the preservation of stoichiometry and the ease to grow multilayered films. These two features enable the growth of multilayered devices of different materials or dopings without the need for residual gases or doping sources; just targets with the desired doping are used. This leads to a reduction in the fabrication time and cost. We have used PLD to fabricate a multi-layered

infrared photodetector that is based on Si/Ge QDs grown on Si(100) substrate.

2. Photodetector Fabrication

Si substrates (p-type, $\sim 5 \times 10^{17} \text{ cm}^{-3}$) are chemically cleaned as described previously [13,14], then loaded into the vacuum chamber. The chamber is pumped down and baked for 12-24 hours before flashing the substrate to $\sim 1100^\circ\text{C}$ in order for the 2×1 reconstruction to develop. The Si substrate is kept at 773 K during deposition in a base pressure $< 1 \times 10^{-9}$ Torr. A 40-ns Nd:YAG laser (0.16 J/cm^2 , 50 Hz) is used to ablate the rotating target, which is in the form of two semi-circular disks placed together to form a circle; one is Si (p-type, $1 \times 10^{19} \text{ cm}^{-3}$) and the other is undoped Ge. Target rotation minimizes the formation of particulates by exposing a fresh area to the laser. The laser is focused on the rotating target with a spot size of $330 \mu\text{m}$ (measured at $1/e$ of the peak value). The system is designed in such a way that the laser hits the target at 45° . A thickness of $\sim 0.6 \text{ nm}$ Ge is first deposited, followed by depositing $\sim 0.4 \text{ nm}$ Si. The process is repeated for 40 revolutions. A Si capping layer of $\sim 1 \text{ nm}$ is deposited before a mask is used to deposit about 100-nm thick Al contacts. The deposition of the 40-layered device, without the metal contacts, took $\sim 500 \text{ s}$, which is much less than the time needed to fabricate similar devices by other deposition techniques. A schematic diagram of the device is shown in Fig. 1.

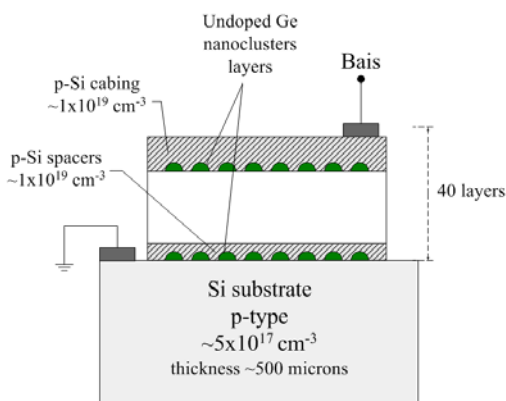


Fig. 1. Schematic of the multi-layered Ge QD-based photodetector grown by PLD on Si(100).

3. Growth Characterization

To monitor the deposition, reflection high-energy electron diffraction (RHEED) is used. During the initial stages of deposition, the Si(100)- 2×1 diffraction pattern, Fig. 2 (left), does not change, which accounts for the formation of the 2D wetting layer. In such 2D growth, the Ge film grows having the Si lattice constant. Upon the completion of the first Ge layer, the RHEED diffraction pattern transforms into a transmission pattern, Fig. 2 (right), indicating the formation of elongated (hut) Ge QDs. Ge QDs form to relieve the internal strain inside the film due to the lattice mismatch between Ge and Si. Such transmission pattern is taken as an indication for the formation of QD to start the deposition of the Si spacing layer. As the capping layer is being grown, the transmission pattern does not change in shape, but decreased in intensity.

The morphology of the Ge film is studied by *ex situ* AFM. For this purpose, a Ge film, of the same thickness of the first QD layer, was grown under the same deposition conditions. Figure 3 shows the formation of the Ge QDs, which are distributed homogeneously over the substrate. A detailed study of the Ge QD formation on Si(100)- 2×1 showed that, under similar deposition conditions at the same thickness hut clusters are formed [13,14]. The size distribution of the Ge QDs of Fig. 3 is shown in Fig. 4, indicating a FWHM of $\sim 35 \text{ nm}$.

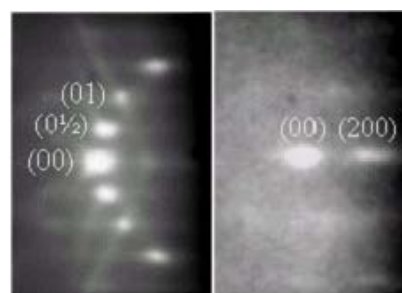


Fig. 2. (Left) RHEED diffraction pattern of the Si(100)- 2×1 substrate. (Right) Transmission pattern formed when the growth of the first Ge QD layer is completed.

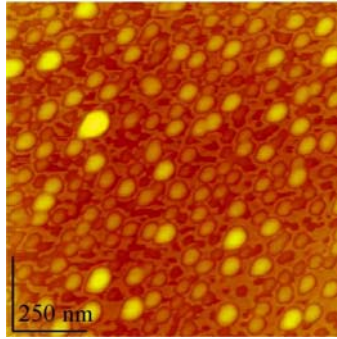


Fig. 3. AFM scan of the Ge quantum dots. The major axis length distribution is shown as inset [scan area = $1.1 \times 1.1 \mu\text{m}$].

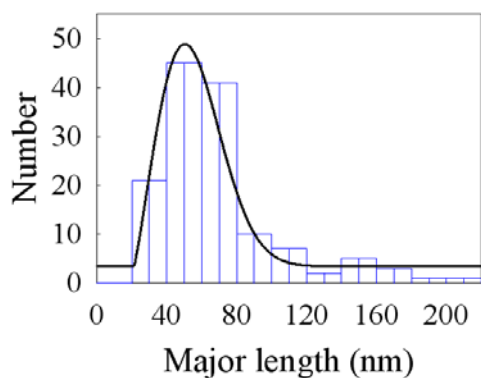


Fig. 4. Histogram showing the size distribution of the above figure.

4. Electrical and Optical Characterization

Silver epoxy was used to mount the QD detector on an Al sample holder and to fix the connecting wires to the Al pads. The sample holder was mounted on the cold-finger of a vacuum sealed cryogenic chamber. The chamber was cooled by liquid nitrogen and the required temperature was obtained using a temperature controller. Vacuum isolation ($\sim 10^{-6}$ Torr) was used with the chamber to preserve temperature stability using a vacuum pumping system. For the spectral response measurements, an optical signal was applied to the detector using the optical section. The optical section consists of a halogen lamp the output of which is modulated using an optical chopper and analyzed using a monochromator. The electrical contacts were integrated to measure the device output for a

certain operating condition. Lock-in amplifier was used to measure the output signal for a given radiation input. A spectrum analyzer was used for noise measurements. A semiconductor characterization system was used for the I-V measurements. All these instrumentation are linked to a personal computer for data acquisition and control. The instruments are synchronized using the chopper controller. A preamplifier is used to convert the detector current into voltage signal. Details on the detector characterization setup are given in [15]

Figure 5 shows the I-V characteristics of the device at different operating temperatures. The I-V characteristics reveal the diode behavior of the sample, which confirms the Schottky structure. Cooling down the device slightly reduces the dark current, suggesting the domination of the leakage current due to the tunneling process. The inset of Fig. 5.9 zooms in to a part of the 293.2 K characteristics. The inset compares the curves obtained in dark and illumination conditions. A current shift of about $5 \mu\text{A}$ with 14.5 W/cm^2 incident intensity suggests the sensitivity of the device to radiation. In order to quantize this sensitivity a spectral response measurements were carried out.

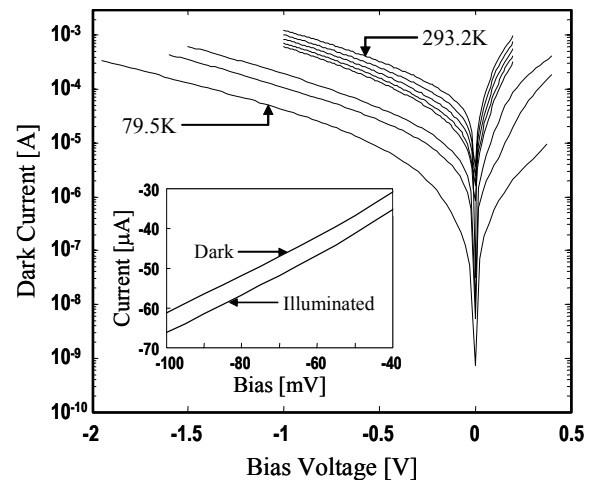


Fig. 5. Dark current variation with bias voltage obtained at temperatures of 293.2, 283.2, 273.2, 263.2, 253.2, 160.0, 130.0 and 79.5 K from top to bottom, respectively. The inset shows a portion of the dark current at 293.2 K and its variation due to device illumination with 14.5 W/cm^2 .

The spectral response of the QD photodetector sample is shown in Fig. 6. The characteristics were obtained in the wavelength range of 1.0 to 3.2 μm at 79.5 K operating temperature and different bias voltages. The spectral range is compatible with the optical section limitation. Lower temperatures have been used to minimize the device noise since the responsivity is low. The spectral response reveals peak responsivity around 2 μm wavelength with ~ 1.8 and ~ 2.2 μm cut-on and cut-off wavelengths, respectively. The presence of this peak is attributed to the type-II band lineup with interband transitions observed in Si/Ge QDs. Tuneability of this peak can be potentially achieved by controlling the composition, size, and size distribution of the QDs through varying the deposition parameters. These deposition parameters include growth temperature, laser fluence and repetition rate, and thickness of the Si spacers. Another possible peak at a longer wavelength with a cut-on around 3 μm is visible in the figure. High responsivity at 1 μm dominates the maximum at 0.5 V due to absorption in the Si substrate. The responsivity increases almost three orders of magnitude (from $\sim 5 \times 10^{-6}$ A/W to $\sim 3 \times 10^{-3}$ A/W at 2 μm) by increasing the bias from 0.5 to 3.5 V. Although this might be attributed to an internal gain mechanism, it is associated with increase in the noise level. In Fig. 7, the noise is plotted against the operating bias voltage. For comparison, the device detectivity (D^*) is plotted in the same figure. Knowing the mean responsivity, R , at a certain bias voltage, and by measuring the noise current density, i_n , at the same voltage the detectivity is calculated using the relation

$$D^* = \frac{i_n}{R} \cdot \sqrt{A},$$

where A is the area of the sensitive element. The figure reveals a poor detectivity compared to typical infrared detectors operating at the same wavelength range, even at room temperature. Nevertheless, the results indicate a potentially promising device, with wavelength tunability option. The poor detectivity is attributed to the poor responsivity associated with QD detectors in general.

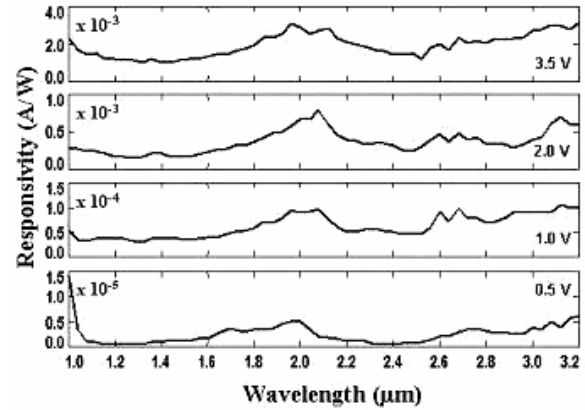


Fig. 6. Spectral response at different bias voltages, obtained at an operating temperature of 79.5 K.

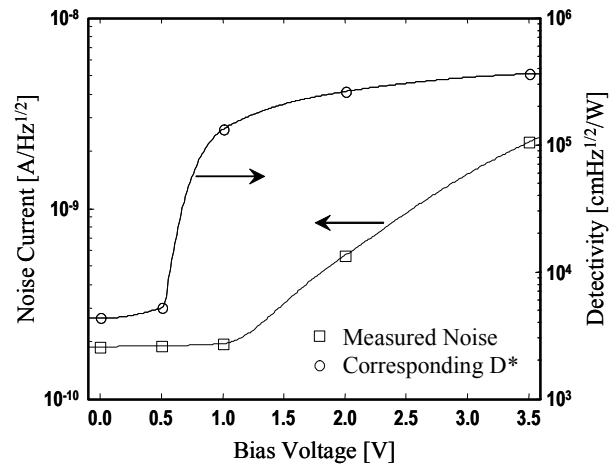


Fig. 7. Measured and fitted noise variation with bias voltage and the corresponding detectivity (D^*), obtained at an operating temperature of 79.5 K.

4. Conclusion

The fabrication of a mid-infrared photodetector by PLD is reported. The device consists of 40 successive Ge QD layers separated by 39 Si spacers and a topmost Si capping layer. The fabrication time of the device, without the metal contacts, takes ~ 500 s. The growth was studied by *in situ* RHEED to identify the formation of Ge QDs, while *ex situ* AFM is used to study the morphology of the QDs and their size and spatial distributions. The difference in the current values in dark and illumination conditions shows the device sensitivity to radiation. Spectral responsivity

measurements reveal a peak around 2 μm , the responsivity of which increases three orders of magnitude as the bias increases from 0.5 to 3.5 V. However, the low detectivity requires some design improvements.

4.1 Acknowledgement

This work was supported by the US Department of Energy, Division of Materials Sciences, under Grant No. DE-FG02-97ER45625.

References:

- [1] V. A. Egorov, G. É. Cirilin, A. A. Tonkikh, V. G. Talalaev, A. G. Makarov, N. N. Ledentosov, V. M. Ustinov, N. D. Zakharov, and P. Werner, "Si/Ge nanostructures for optoelectronics applications," *Phys. Solid State* 46(1), 2004, pp. 49-55.
- [2] A. Elfving, G. V. Hansson, and W.-X. Ni, "SiGe (Ge-dot) heterojunction phototransistors for efficient light detection at 1.33-1.55 μm ," *Physica E*, 16, 2003, pp. 528-532.
- [3] J. L. Liu, A. Khitun, K. L. Wang, T. Borca-Tasciuc, W. L. Liu, G. Chen, and D. P. Yu, "Growth of Ge-Quantum Dot Superlattices for Thermoelectric Applications," *J. Cryst. Growth* 227-228, 2001, pp. 1111-1115.
- [4] A. Alguno, N. Usami, T. Ujihara, K. Fujiwara, G. Sazaki, K. Nakajima, and Y. Shiraki, "Enhanced quantum efficiency of solar cells with self-assembled Ge dots stacked in multilayer structure," *Appl. Phys. Lett.* 83, 2003, pp. 1258-1260.
- [5] V. Ryzhii, "The theory of quantum quantum-dot infrared phototransistors," *Semicond. Sci. Technol.* 11, 1996, pp. 759-765.
- [6] M. Maksimović, "Quantum dot infrared photodetector as an element of free-space optics communication systems," XI Telekomunikacioni Forum Telefor, 2003.
- [7] E. Towe and D. Pan, "Semiconductor quantum-dot nanostructures: their application in a new class of infrared photodetectors," *IEEE J. Sel. Top. In QE* 6(3), 2000, pp. 408-421.
- [8] H. C. Liu, "Quantum dot infrared photodetectors," *Optoelectronics Rev.* 11(1), 2003, pp. 1-5.
- [9] C. Miesner, O. Röthing, K. Brunner, G. Abstreiter, "Mid-infrared photocurrent measurements on self-assembled Ge dots in Si," *Physica E* 7, 2000, pp. 146-150.
- [10] K. Brunner, "Si/Ge nanostructures," *Rep. Prog. Phys.* 65, 2002, pp. 27-72.
- [11] V. Cimalla, K. Zekentes, and N. Vouroutzis, "Control of morphological transitions during heteroepitaxial island growth by reflection high-energy electron diffraction," *Mater. Sci. Eng. B* 88, 2002, pp. 186-190 (2002).
- [12] P. S. Chen, Z. Pei, Y. H. Peng, S. W. Lee, M.-J Tsai, "Boron mediation on the growth of Ge quantum dots on Si (100) by ultra high vacuum chemical vapor deposition system," *Mat. Sci. Eng. B* 108, 2004, pp. 213-218.
- [13] M. S. Hegazy and H. E. Elsayed-Ali, "Self-assembly of Ge quantum dots on Si(100) by pulsed laser deposition," *Appl. Phys. Lett.* 86, 2005, 243204.
- [14] M. S. Hegazy and H. E. Elsayed-Ali, "Growth of Ge quantum dots on Si by pulsed laser deposition," *J. Appl. Phys.* 99, 2006, 054308.
- [15] T. F. Refaat, M. N. Abedin, O. V. Sulima, U. N. Singh and S. Ismail, In *IEDM Tech. Dig.*, 2004, pp. 355-358.